

## The Antibacterial Efficacy of Antibiotic-Loaded Mesoporous Silica Nanoparticles

Samar M. Alhabardi

Faculty of Science for Girls, King Abdulaziz University, Jeddah, Saudi Arabia Kingdom  
[sunstar33@windowslive.com](mailto:sunstar33@windowslive.com)

**Abstract:** In recent years, several studies have been developed to control drug delivery and reduce the toxicity of drugs as well as to create novel biomedical applications. Mesoporous silica nanoparticles (MSNs) have attracted the attention of many researchers, who have studied these materials for use in many applications. MCM-41 particles have a unique pore size, a higher surface area, and are a good matrix for guest–host applications. The aim of this work is to study the efficacy of antibiotic-loaded MSNs. The MSNs particles were synthesized using a liquid crystal templating method, with n-cetyltrimethylammonium bromide (CTAB) as the surfactant template and tetraethyl orthosilicate (TEOS) as the silica source. These mesoporous materials were characterized using a Fourier transform infrared spectroscopy, scanning electron microscopy, transmission electron microscopy (TEM), high-performance liquid chromatography, nitrogen adsorption/desorption, and dynamic light scattering. Amoxicillin and erythromycin were used as the model drugs. The antibacterial effect and mechanism of the MSNs was investigated for Gram-positive *Staphylococcus aureus* (*S. aureus*) and Gram-negative *Escherichia coli* (*E. coli*) using time-kill assay testing. The results of the present study clearly showed a significant reduction in *S. aureus* after treatment with antibiotic-loaded MSNs. However, there was no significant reduction observed against *E. coli* after treatment with amoxicillin-loaded MSNs. This difference may be a result of the mode of action of bacteria. In addition, TEM analyzed the bacteria treated with antibiotic-loaded MSNs. This study could contribute to a new antibacterial treatment and could lead to a reduction in the toxicity of drug in the future. Drug delivery systems have valuable applications in various fields; however, further investigation is required in many areas, including neurosciences, cancer, and biomedical engineering.

[Samar M. Alhabardi. **The Antibacterial Efficacy of Antibiotic-Loaded Mesoporous Silica Nanoparticles.** *Life Sci J* 2016;13(6):31-39]. ISSN: 1097-8135 (Print) / ISSN: 2372-613X (Online). <http://www.lifesciencesite.com>. 4. doi:[10.7537/marslsj13061604](https://doi.org/10.7537/marslsj13061604).

**Key words:** Mesoporous silica nanoparticles, nanoparticles, MCM-41, drug delivery systems, *Staphylococcus aureus*, *Escherichia coli*, Amoxicillin, erythromycin

### 1. Introduction

In recent years, Mesoporous silica nanoparticles (MSNs) have attracted more attention due to their broad range of applications (He *et al* 2011). Because of their unique characteristics, mesoporous materials are attractive materials for applications such as catalysis, adsorption, separation and sensing and drug delivery devices (Rosenholm and Linden, 2008). Nanoparticles, after functionalisation and combination with other types of material, have recently been demonstrated to be good contrast agents in magnetic resonance imaging (Tao *et al.*, 2009; He *et al.*, 2011). These materials have demonstrated excellent biomineralisation ability and capacity for controlled drug release. Moreover, MSNs have been applied to scaffolds as a potentially degradable means of drug delivery for bone tissue regeneration. After immobilisation of an antibiotic, they can be used successfully as a scaffold in bone replacement (Shi *et al.*, 2009). MCM-41, the most widely studied of M41S materials, exhibits hexagonal arrays of cylindrical mesopores. Thanks to its simple synthesis, it is probably the material most often used to compare with other materials or to apply in areas such

as catalysis, sorption, sensing and inclusion chemistry (Vadia and Rajput, 2011; Zhao *et al.*, 2013).

Now, more and more new methods have been developed for synthesising a variety of MSNs, which can be done under controlled laboratory conditions (de Sousa *et al.*, 2010). MCM-41 materials are synthesised by a method that has become known as liquid crystal templating (LCT) (Beck *et al.*, 1992; Kresge *et al.*, 1992). With CTAB as a surfactant template and tetraethylorthosilicate (TESO) or sodium metasilicate ( $\text{Na}_2\text{SiO}_3$ ) as the silica, MCM-41 displays a lyotropic mesophase in water (Meynen *et al.*, 2009). The surfactant template can be removed either by using chemical extraction or by calcination.

Currently, several materials are being studied for their potential to prepare drug delivery systems and to control their delivery (Barba *et al.*, 2005). In comparison to conventional drug dosages, it is possible to change the pharmacokinetics of a drug and to control its delivery by using an effective drug delivery system (DDS). Whereas the traditional dosage could cause side effects, these side effects may be eliminated or reduced by using DDSs (Vallel-Regi *et al.*, 2007), which have various benefits for therapeutic efficacy and reducing

toxicity, as well as reducing the number of drug doses required.

Nowadays, several studies are focused on preparing mesoporous materials for drug delivery that can store large amounts of drugs and are able to control delivery and release the drug slowly over an extended time. (Oye *et al.*, 2011; Shi *et al.*, 2001).

Pore size can play an important role in the drug release kinetics, especially if the drugs have a similar size to the pore diameter of the MSNs (Vadia and Rajput *et al.*, 2011; Tang *et al.*, 2012). The drug loading process is mainly based on the surface area and pore diameter, which are the most critical factors determining the amount of adsorbed drug (Horcajada *et al.*, 2004; Izquierdo-Barba *et al.*, 2005). However, by increasing or reducing the surface area or by modifying the surface-dry affinity, the amount of drug adsorbed may result in greater drug loading (Vallet-Regí *et al.*, 2006). After the first study in 2001 by Vallet-Regí, a large number of investigations have focused on developing a structurally stable drug delivery system that can carry a large number of drug molecules without incurring any problem of premature release.

In this study, amoxicillin and erythromycin are the main antibiotics of interest as model drugs for drug-loading, as they have different structure and molecular mass.

The molecular mass of erythromycin is much larger than that of amoxicillin and its width is 14.38 Å. MCM-41 has been used in many experiments as a drug carrier, including erythromycin, for drug loading.

The purpose of this study was to investigate the molecular mass and size of these antibiotics in order to determine if they have an effect on drug loading and release.

Studies of the interaction of MSNs with bacteria are rare and many aspects of the interaction have still not been investigated. Several researchers have studied many aspects of MSNs from animal cells (Lensing *et al.*, 2013), notably morphological aspects such as particle size (Lu *et al.*, 2009), and surface modifications (Slowing *et al.*, 2006). The results of these studies have shown the possibilities of MSNs as drug carriers.

In this study, two types of bacteria were used: *staphylococcus aureus* NCTC 6571 (*S. aureus*) as the Gram-positive model, and *Escherichia coli* NCTC-9001 (*E. coli*) as the Gram-negative model.

MSNs as antimicrobial agents were investigated by growing *E. coli* and *S. aureus* on nutrient agar plates and comparing them with blank MSNs. These bacteria have marked differences between their cell walls. A Gram-positive bacterium has a much thicker cell wall than a Gram-negative bacterium. This thicker cell wall of *S. aureus* may play an essential role in protecting the

cell from antibiotics and in affecting the efficacy of MSNs.

## 2. Experiments

### Synthesis of mesoporous silica nanoparticles

n-cetyltrimethylammonium bromide (CTAB) and tetraethylorthosilicate (TEOS) were obtained from Sigma and used without further purification. Cetyltrimethylammonium bromide (CTAB, 1.0 g,  $2.74 \times 10^{-3}$  mol) was dissolved in 480 mL of deionised water at room temperature. An aqueous solution of NaOH (2M, 3.5 mL) was added dropwise to the CTAB solution. The temperature of the solution mixture was increased to 80°C, followed by dropwise additions of TEOS (5 mL, 2.57-tO--rnoaln), which was used as the silica source. The reaction mixture was stirred for 2h. The solid products were isolated by filtration. The surfactant was removed by calcination of the filtered product for 4h 30 min at 873K.

### Characterisation

The samples were characterised before and after the calcinations. The FTIR spectra were obtained at room temperature. 0.0025 g from MSNs were used with KBr pellets.

The nitrogen adsorption-desorption measurements were completed using a Micromeritics ASAP 2020 surface area and porosity analyser. Prior to measurement, the sample was outgassed overnight under high vacuum pressure at around 200°C to remove water from it. The specific surface areas were calculated using the Brunauer-Emmett-Teller (BET) method and pore size was calculated using desorption branches of the isotherm by the Barrett-Joyner-Halenda (BJH) method.

Dynamic light scattering (DLS) was used to obtain the hydrodynamic size distribution of MNPs. Zeta-potential was calculated by laser Doppler electrophoresis (LDE). Temperature was set at 298K, and the MNPs dispersed in water.

The particle morphology of these MSN materials was determined by scanning electron microscopy (SEM) using a JEOL JSM-5600 LV scanning electron microscope with 20 kV accelerating voltage and 0.005 nA of beam current for imaging. Images were taken at magnifications ranging from 20,000 to 40,000x.

The instrument used for the TEM analysis was a Philips TECNAI 12 BioTWIN transmission electron microscope, with electron optical magnification of 45,000. A growth curve was determined for bacteria *E. coli* and *S. aureus*. The growth of bacteria was measured with a spectrophotometer corresponding to  $10^5$  CFU/ml at 600 nm. The lag phase of *E. coli* was 20 min and for *S. aureus* 30 min.

A zone of inhibition was prepared for both amoxicillin and erythromycin antibiotics at the same

concentrations. For concentrations from 1500 to 2  $\mu\text{g}/\text{mL}$ , the drugs were dissolved in distilled water.

A zone of inhibition was prepared for both amoxicillin- and erythromycin-loaded MNPs at the same concentrations. MNPs (0.2g) were loaded with antibiotics separately (1500  $\mu\text{g}/\text{mL}$ ; 5 mL) and dissolved in methanol (80%) by shaking (200 rpm) the suspension for 48 h. The product was collected by centrifugation (5000 rpm/ 20 min) and dispersed in distilled water (5 mL). The same procedure was utilised for MNPs loaded with antibiotics at 500  $\mu\text{g}/\text{mL}$ .

#### Time-kill antibacterial assay

A time-kill assay was prepared for both antibiotics at the same concentration. MNPs (0.2 g) were soaked in antibiotics separately (1500  $\mu\text{g}/\text{mL}$ ; 10 mL) and dissolved in methanol by shaking (200 rpm) the suspension for 48 h. The product was collected by centrifuge (5000 rpm/ 20 min). MNPs containing the antibiotics dispersed in nutrient broth (2 mL) were dispersed in broth (1 mL) containing bacteria. The overall CFU in the suspension was  $1 \times 10^6$ . The suspension was incubated at  $37^\circ\text{C}$ , and shaken 20 min for *E. coli* 20 min and 10 min for *S. aureus* (depending on the result before). Then at regular time intervals, aliquots (50  $\mu\text{L}$ ) were plated on to nutrient agar plates and incubated at  $37^\circ\text{C}$  for 24 h. The same procedure was used for both amoxicillin and erythromycin when loading the MNPs with a concentration of 500  $\mu\text{g}/\text{mL}$ .

All microbiological experiments were repeated three times and the results and data points are presented as mean averages.

For TEM analysis, a sample of bacteria was treated with MSNs dispersed within glutaraldehyde fixative and left for a day. The solution was collected by centrifuge at 2000 rpm for 5 min, after which a 0.5 ml wash buffer was added.

### 3. Results and Discussion

#### Characterisations

Following the synthesis, the MSNs were characterised, and several techniques were used to determine particle and pore morphology, structure and surface details.

#### Particle size and Zeta-potential measurement

The dynamic light scattering (DLS) technique was used to provide information about particle size. The particle size distribution of MSNs, having an average size of 90 nm ; those observed here were similar to those seen in the calculations using the BJH model.

#### Scanning and transmission electron microscopy (SEM/TEM)

Electron microscope measurement was used to establish the particle morphology and examine particle diameter and particle size distribution.

Images obtained by SEM (Figures 1 a and b) provided information on the physical properties of MSNs and particulates, including particle size, shape and surface morphology.

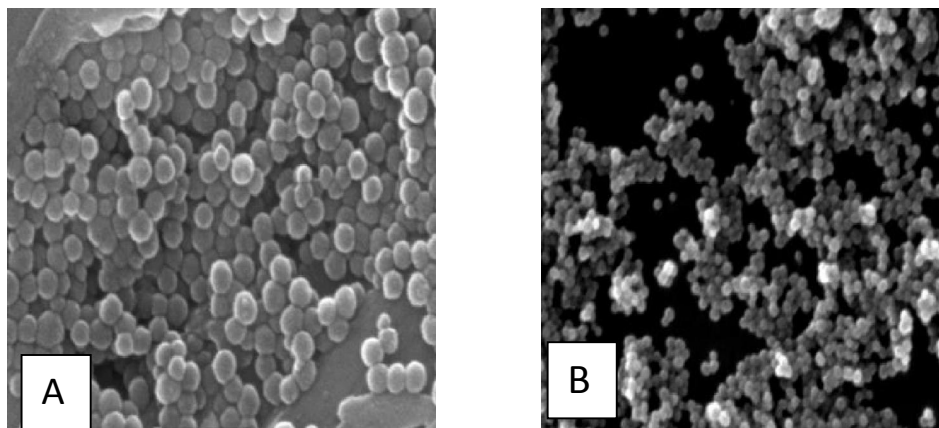


Figure 1: SEM micrographs of MSNs. a) Before template removal x40k magnification b) After template removal x20k magnification.

The SEM measurement show agglomerated particles, which were relatively uniformly shaped spheres with a size of  $<100\text{ nm}$ . SEM was performed on the MSNs before and after removing the template. MSNs appeared to have aggregated together, which may have been due to a high concentration that dried on the SEM stub. Typical SEM data obtained for

MSNs area shown before removal of the template and after calcination. As may be seen, there are no differences in the MSNs without the template: the uniformly spherical structure is identical.

Transmission electron microscopy (TEM) was additionally used to confirm the morphology of MSNs; its advantage is that it shows the sample as a whole as

well as what is inside or beyond the surface (Santini *et al.*, 2000), whereas SEM focuses on the sample's surface and its composition. MSN was successfully synthesised according to the TEM images. As may be seen in Fig. 2, TEM demonstrated the high mesoporosity of MCM-41 and that the mesopore possesses a highly ordered hexagonal array of uniform channels with curved and rectilinear morphologies.

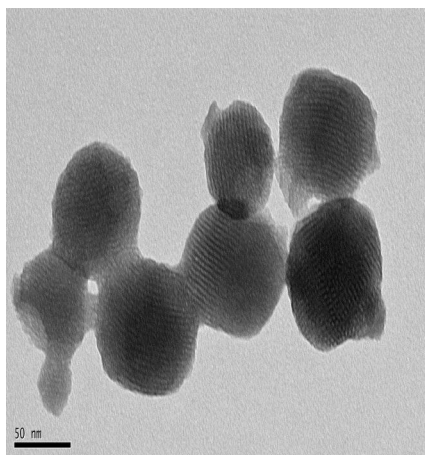


Figure 2: TEM micrographs of calcined MSNs

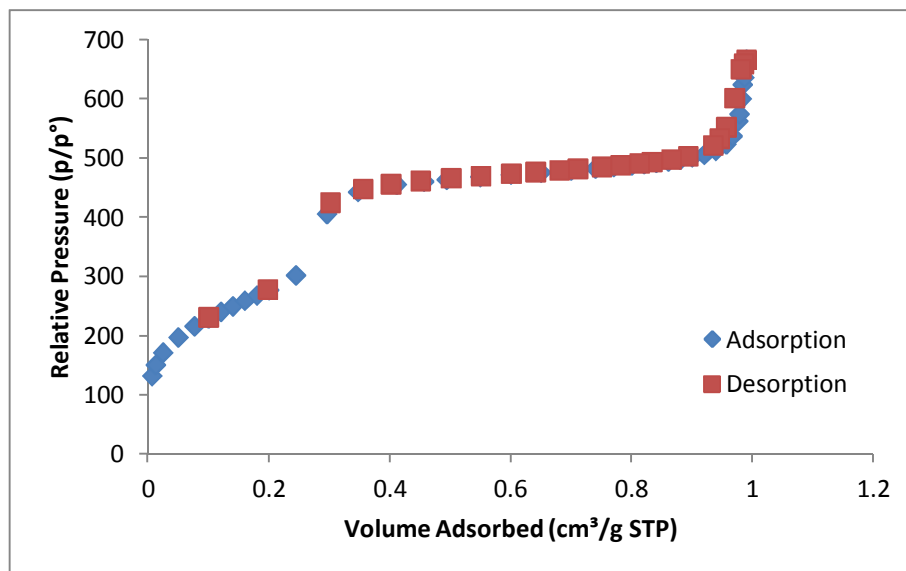


Figure 3: BET isotherm of mesoporous silica nanoparticles.

The total surface area of the calcined MCM-41 particles was calculated by the Brunauer-Emmett-Teller (BET) method and found to be  $1207.2906 \pm 99.5067$  m<sup>2</sup>/g. The average pore diameters calculated using the BJH model for MCM-41 were centred around 2.2 nm as one sharp peak (Figure 4), which is the most common pore size for this type of material. The pore diameter of mesopores according to IUPAC is between 2 nm and 50 nm (Sing *et al.*, 1985). Therefore, the

Therefore, the structure of MCM-41 is of particular interest because its pore size distribution and straight unconnected channels make it an ideal adsorbent for fundamental theoretical research and an ideal host for large molecules (Garcia - Bennett *et al.*, 2004). The hexagonal array morphology is highly ordered and stable. The scale bar of the micrographs was 50 nm.

#### Nitrogen Adsorption and Desorption Isotherms

In order to understand the behaviour of the mesoporous material in future applications, nitrogen adsorption isotherms were used to provide information about the surface area, median pore diameter and pore volume. The nitrogen adsorption-desorption isotherms and pore size distributions (PSDs) of the MCM-41 after template removal are shown in Fig.3 and Fig. 4. The shape of the isotherm was determined as type IV, according to IUPAC nomenclature, which confirms the presence of a mesoporous structure. According to the graph, the steep lines and the present system hysteresis loops were observed to be approximately 0.25 P/P<sub>0</sub>, which is also the pore-filling step. This is similar to most of the isotherms reported in the literature.

material synthesised is accurately described as mesoporous. The pore size distribution using the BJH methods agreed very well with estimated pore sizes from the TEM results. These results were expected for MCM-41.

Moreover, it has been suggested that this material is able to carry the drug molecules used in this project, since the pore size of MSN is larger than that of amoxicillin (13.94 Å) and erythromycin (14.38 Å)

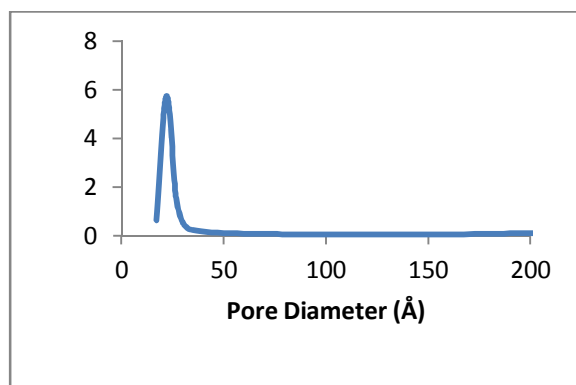


Figure 4: Pore size distribution of mesoporous silica nanoparticles.

#### Zone of inhibition of antibiotic-loaded MSNs

A test was performed of the antimicrobial efficacy of MSNs against both Gram-positive and Gram-negative bacteria. Two concentrations were examined, namely 500 and 1355  $\mu\text{g}/\text{mL}$  of amoxicillin and erythromycin, selected according to the results from the zone of inhibition test with antibiotics. The effect was more noticeable for erythromycin against *S. aureus* than against *E. coli*, as the MSNs with antibiotic were able to inhibit the growth of organisms (Fig. 5).

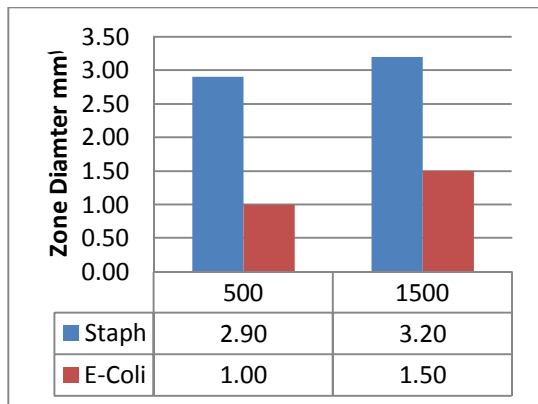


Figure 5: Zone of inhibition erythromycin-loaded MSNs.

On the other hand, amoxicillin displayed no inhibition zone against the growth of *E. coli*; hence it was considered to be resistant against this antibiotic, whereas at a high concentration of 1355  $\mu\text{g}/\text{mL}$  the zone was only slightly effective against *S. aureus*. The explanation for this is that *E. coli* have an extra outer membrane, which can make the bacteria more resistant to drugs and may also affect the ability of the particles to be internalised (Fig. 6).

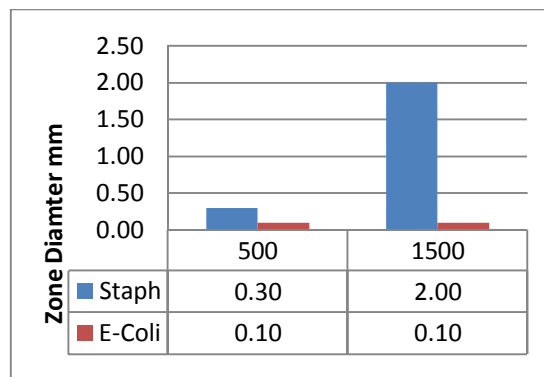


Figure 6: Zone of inhibition with amoxicillin

Comparing the results from zone of inhibition antibiotics and zone of inhibition of antibiotics loaded with MSNs shows a difference in the effectiveness of the amoxicillin-only and amoxicillin-loaded MSNs against *E. coli*. The effectiveness of amoxicillin-only reduced when MSNs were loaded, which may be due to the particularly delayed release of the amoxicillin molecule. This delay may have allowed the bacteria to proliferate. Overall, the level of effectiveness for both amoxicillin- and erythromycin-loaded MSNs against *S. aureus* and *E. coli* was lower compared with the antibiotic only.

#### Time-kill antibacterial assay

Time-kill assay was used to show the efficacy of the antibiotic-loaded MSNs and provide general rate-of-kill information. Mean colony counts were plotted against time. Recent research has developed an explanation of the effect of antibiotic-loaded MSNs inhabiting the bacteria.

The time-kill experiment in this study observed no antibacterial activity, as was shown by using plain MSNs. As expected, the bacteria multiplied greatly. Time-kill studies at 5 min, 0.5, 1, 3, 6 and 24h have shown that antibiotic-loaded MSNs were able to significantly decrease the number of colonies throughout the 24h period of incubation for both antibiotics against *S. aureus*. Likewise, there was a significant decrease in the growth of *E. coli* with erythromycin-loaded MSNs (Fig. 7).

However, there was no antibacterial activity with amoxicillin-loaded MSNs against *E. coli* at 24h, which appeared similar to the control (Fig. 8).

This result was expected because it was similar to that of zone of inhibition with MSNs. The results from the zone of inhibition indicate that amoxicillin-only was able to inhibit *E. coli*. Thus, MSNs may have affected amoxicillin's ability to inhabit the bacteria. The surfaces of *E. coli* cells have a negative net charge and, as already mentioned, the negative charge of MSNs (after template removal) may cause the bacteria to become resistant. In addition, the attraction between the net charge of the bacterial cell and the net charge of

nanoparticles is crucial for the activity of nanoparticles. Amoxicillin is very active against Gram-positive organisms, whereas *E. coli* is regarded as Gram-negative, which may account for the resistance. Although amoxicillin can be effective in inhibiting other Gram-negative bacteria, it may be that the *E. coli* strain that was used in this study had developed a resistance to this particular antibiotic. Moreover, the outer membrane of *E. coli* cells, which is predominantly constructed from tightly packed LPS molecules, make the bacteria more resistant.

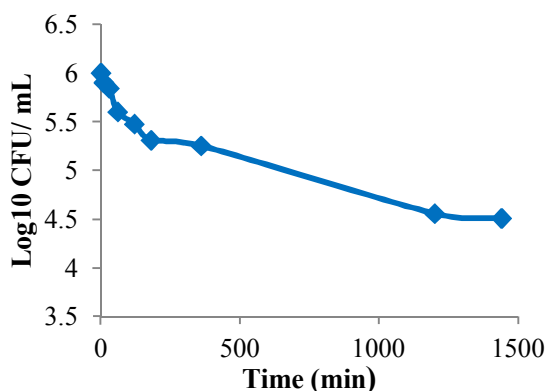


Figure 7: Growth curve of *E. coli* treated with erythromycin-loaded MSNs.

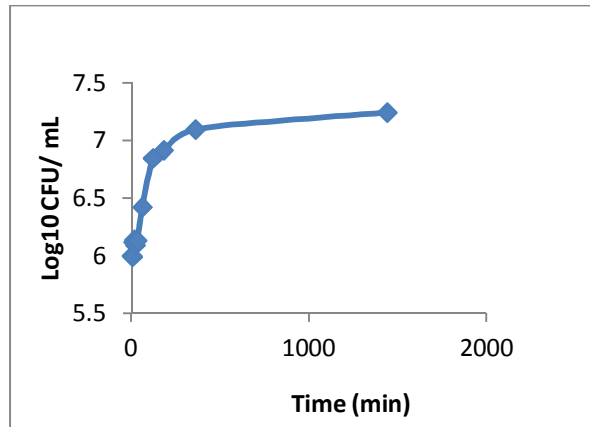


Figure 8: Growth curve of *E. coli* treated with amoxicillin-loaded MSNs.

It is of note that the erythromycin-loaded MSNs significantly inhibited the number of *S. aureus* bacteria, starting at 10 min, and over time the number of *S. aureus* colonies decreased, the most noticeable reduction being after 24h, when no bacteria colonies could be detected (Fig. 9). Since erythromycin is known to be effective against Gram-positive organisms, this observation is in keeping with expected results.

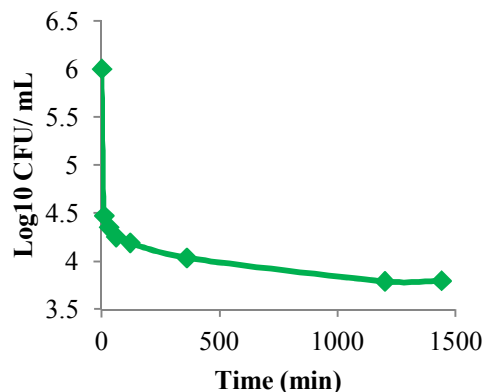


Figure 9: Growth curve of *S. aureus* treated with erythromycin-loaded MSNs

By contrast, the amoxicillin-loaded MSNs did not show a noticeable effect on *S. aureus* growth compared with erythromycin-loaded MSNs; the growth of bacteria started to decrease at 3h and the number of colonies declined at 24h (Fig. 10). It is worth noting that the majority of *S. aureus* produce beta-lactamase, an enzyme that works to protect *S. aureus* against amoxicillin, as it has the ability to break the beta-lactam ring in the structure of amoxicillin by hydrolysis. Therefore, amoxicillin is susceptible to degradation by *S. aureus* to varying degrees, whereas *E. coli* has developed resistance to amoxicillin. Today, this mode of action has become a major clinical problem (Vallet-Regi *et al.*, 2004). The present study indicates that it is possible to suppress bacterial proliferation for up to a day by mesoporous silica loaded with erythromycin against *S. aureus*. In addition, it suggests that MSNs may work against resistance of the bacteria and thus pave the way for novel antibacterial treatments.

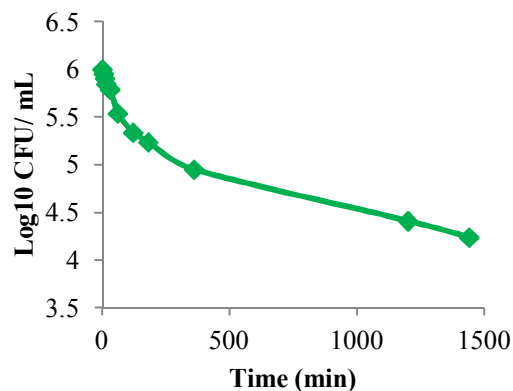


Figure 10: Growth curve of *S. aureus* treated with amoxicillin-loaded MSNs.

Thanks to the structure of MSNs, especially their pores, which are bigger than bacteria, the chance of contact between antibiotics and bacteria increases. This can improve the efficiency of antibiotics and lead to the widespread utilisation of mesoporous material in all fields.

The main factor that can affect the drug-loading process is the adsorptive properties of mesoporous material (Stromme *et al.*, 2008; Wang., 2009). Therefore, the surfaces of MSNs become the most significant factor for the amount of adsorbed drug (Zhao *et al.*, 1998). Furthermore, several other factors can influence mass transfer in the loading system, such as pore size and shape. As mentioned above, the pore size and shape estimated from TEM images and the data from nitrogen isotherms reveal the ability of MSNs to carry antibiotics. Further, the crystallization of the drug can hinder and even stop the process of drug loading, as it tends to cause blocking of the pores of the mesoporous material. However, both antibiotics used in the present study, amoxicillin and erythromycin, can be readily loaded in the pores of MSNs.

Several studies have shown that cationic particles have a greater affinity towards the negatively charged lipo-polysaccharide layer that coats such Gram-negative bacteria as *E. coli*. On the other hand, the negative charge of MSNs is more effective in slowing the growth of *S. aureus*.

The time-kill curve also suggests that the amoxicillin-loaded MSNs' ineffectiveness against *E. coli* may be due to the fact that the dose of amoxicillin released was not enough to inhibit this particular bacterium. However, an increased amoxicillin dose would be toxic to the patient.

#### **Morphological changes in bacteria after antibiotic-loaded MSNs treatment**

A transmission electron microscope was used to examine untreated bacteria and showed the external morphological features of *E. coli* cells and their normal morphology of a multilayered cell surface consisting of an outer membrane, a peptidoglycan layer and a cytoplasmic membrane (Fig. 11 a). As can be seen, after antibiotic-loading MSNs treatment, the bacteria became surrounded by nanoparticles (Fig. 11 b).

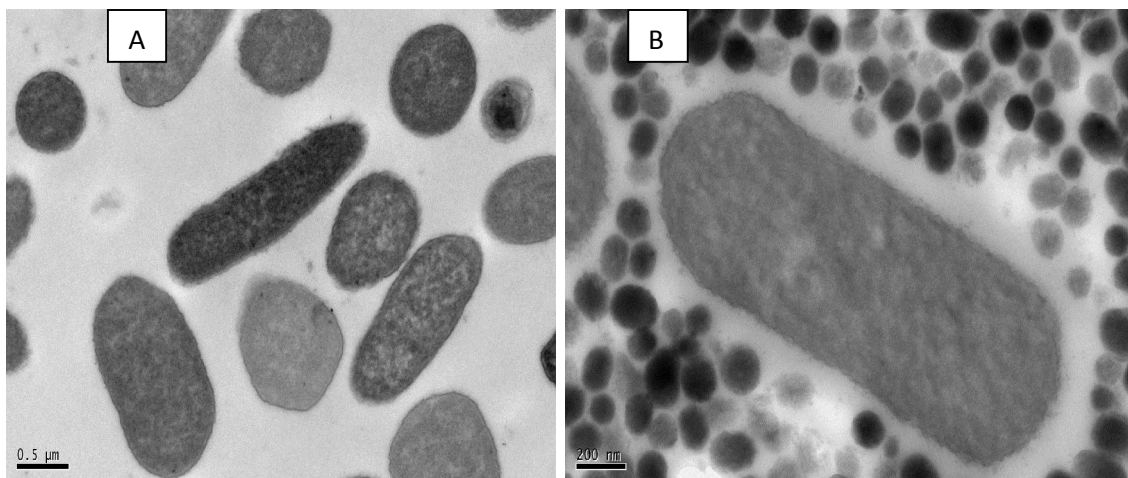


**Figure 11: Internal structure of *E. coli* observed by TEM. a) Untreated bacteria b) After loading of antibiotic.**

However, significant morphological changes were observed in *E. coli* cells after antibiotic-loaded MSNs treatment for 6h; indeed, they appeared to be seriously damaged (Fig. 12 a and b). The cells were cracked and ruptured and cellular contents were released from the cell wall into the surrounding environment, before the cell wall was finally degraded. As can be seen, clear black circles (MSNs) have been internalised by *E. coli* cells within the confines of the cell wall.

The phenomena suggest possible antibacterial mechanisms by which antibiotic-loaded MSNs inhibit bacteria. Furthermore, the interaction between antibiotic-loaded MSNs and the constituents of the

bacterial membrane cause morphological changes and disrupt the membrane and intercellular metabolic activity, which may cause cell death. Although the mechanisms underlying the antibiotic-loaded MSNs are still not fully understood, the internalisation is clear, as shown by the black circles. Figure 12 indicates that not all particles internalised the bacteria. This suggests that the interaction between the bacteria and nanoparticles depends on the size of the particles: small particles were taken up by the bacteria, while large particles were not. TEM micrographs show amoxicillin-loaded MSNs against *E. coli*.

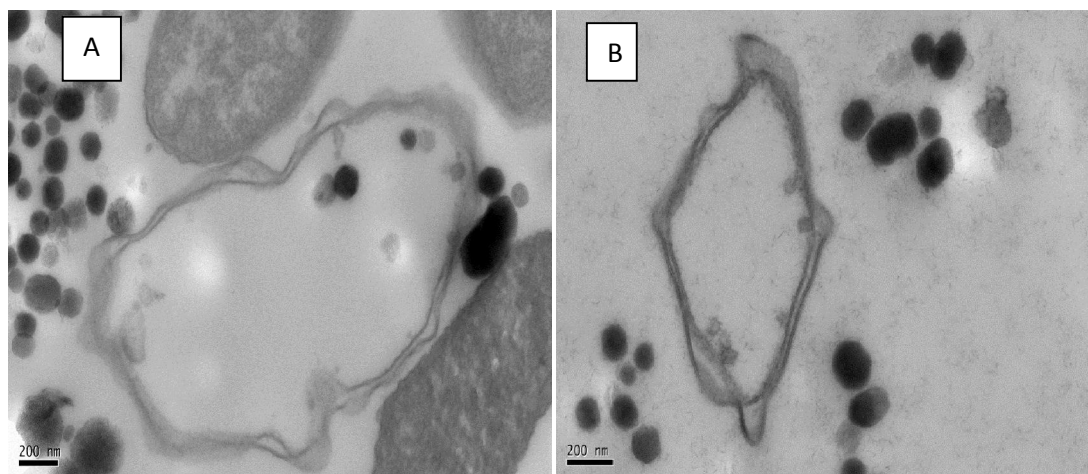


**Figure 12: TEM micrographs of *E. coli* treated with antibiotic-loaded MSNs. The cell was seriously damaged.**

### Conclusion

MSNs were used as hosts and the erythromycin and amoxicillin as guests. The efficacy of antibiotic-loaded MSNs showed a significant decrease in the growth of bacteria, except amoxicillin-loaded nanoparticles against *E. coli*. Interestingly, results from TEM micrographs for *E. coli* treated with antibiotic-loaded MSNs showed the internalisation of the amoxicillin-loaded nanoparticles.

In recent years, MSNs have attracted much attention for their potential for direct drug delivery. Moreover, MSN-based drug delivery offers many benefits. However, many aspects still need to be further more investigated and more studies of bacteria conducted. Such research could open the door to new methods of dealing with the resistance to bacteria by nanoparticles.

### References

1. Barba, II., Martinez, Á., Doadrio, AL., Pariente, JP., and Vallet - Regí, M. (2005) "Release evaluation of drugs from ordered three - dimensional silica structures". *Eur J Pharm Sci*; 26: 365 - 373.
2. Beck, J., Vartuli, J., Roth, W., Leonowicz, M., Kresge, C., Schmitt, K., Chu, T., Olson, D., and Sheppard, E. (1992) "A new family of mesoporous molecular sieves prepared with liquid crystal templates" *Journal of the American Chemical Society*. 114 (27), 10834-10843.
3. de Sousa, A., Maria, D. A., de Sousa, R. G., & de Sousa, E. M. (2010). "Synthesis and characterization of mesoporous silica/poly(N-isopropylacrylamide) functional hybrid useful for drug delivery". *J Mater Sci*, 45, 1478 - 1486.
4. Garcia - Bennett, A., Terasaki, O., Che, S., and Tatsumi, T. (2004) "Structural investigations of AMS - n mesoporous materials by transmission electron microscopy". *Chem Mater*, 16; 813 - 821.
5. He, Q., Shi, J. C., Wei, C., Zhang, L., Wu, W., and Bu, W. (2011). "Synthesis of oxygen deficient luminescent mesoporous silica nanoparticles for synchronous drug delivery and imaging". *Chem. Commun.*, 47, 7947 - 7949.
6. Horcajada, P., Ramila, A., Perez-Pariente, J., and Vallet-Regi, M. (2004) "Influence of pore size of MCM-41 matrices on drug delivery rate", *Micropor. Mesopor. Mater.* 68:105–109. *Int. Ed.*, 39, 2396-2047.
7. Izquierdo-Barba, I., Martinez, A., Doadrio, A. L., Perez-Pariente, J., and Vallet-Regi, M. (2005). "Release evaluation of drugs from ordered three-dimensional silica structures". *European Journal of Pharmaceutical Sciences*, 26, 365 - 373.
8. Kresge, C., Leonowicz, M., Roth, W., Vartuli<sup>h</sup> J., and Beck J. (1992) "Ordered mesoporous molecular sieves synthesized by a liquid-crystal template mechanism" *Nature*, 359, 710 – 712.
9. Lensing, R., Bleich, A., Smoczek, A., Glage, S., Ehlert, N., Luessenhop, T., behrens, P., Muller, P., Kietzmann, M., and Stieve, M. (2013) 'Efficacy of nanoporous silica coatings on middle ear prostheses as a delivery system for antibiotics: An animal study in rabbits' *Acta Biomaterialia*. 9, 4815-4825.
10. Lu, F., Wu, S., Hung, Y., and Mou, C. (2009) "Size Effect on Cell Uptake in Well-Suspended, Uniform Mesoporous Silica Nanoparticles" *Small Journal*, 1-6.
11. Meynen, V., Cool, P., and Vansant, E. F. (2009). "Verified synthesis of mesoporous Materials". *Microporous and Mesoporous Materials*, 125, 170 - 223.
12. Oye, G., Sjoblom, J., and Stocker, M. (2001) "Synthesis, characterization and potential

- applications of new materials in the mesoporous range". *Adv. Colloid Interface Sci.* 89, 439–466.
13. Rosenholm, J. M., and Lindén, M. (2008). "Towards establishing structure activity relationships for mesoporous silica in drug delivery applications." *Journal of Controlled Release*, 128, 157–164.
  14. Santini, J, Schumacher, K., Ravikovitch, B., Du Chesne, A., Neimark, V., and Unger, K. (2000). "Characterization of MCM-48 materials" Microchips as Controlled Drug Delivery Devices". *Angew. Chem. Langmuir* 16, 4648.
  15. Shi, G., Guo, Q. Z., Liu, Y. T., Xiao, Y. X., and Xu, L. (2011). "Drug delivery devices based on macroporous silica spheres". *Materials Chemistry and Physics*, 126, 826–831.
  16. Shi, X., Wang, Y., Ren, L., and N., Z. (2009). "Novel mesoporous silica - based antibiotic releasing scaffold for bone repair". *Acta Biomaterialia*, 5, 1697 - 1707.
  17. Sing, K., Everett, D., Haul, R., Moscou, L., Pierotti, R., Rouquerol, J., and Siemieniewska, T. (1985) "REPORTING PHYSISORPTION DATA FOR GAS/SOLID SYSTEMS with Special Reference to the Determination of Surface Area and Porosity" *International Union of Pure and Applied Chemistry*. 57 (4), 603-619.
  18. Slowing, I., Trewyn, B., and Lin, V. (2006) "Effect of Surface Functionalization of MCM-41-Type Mesoporous Silica Nanoparticles on the Endocytosis by Human Cancer Cells" *American Chemical Society*. 128, 14792-14793.
  19. Strømme, M., Brohede, U., Atluri, R., Garcia-Bennett, A. (2008) "Mesoporous silica - based nanomaterials for drug delivery: evaluation of structural properties associated with release rate" *Nanomedicine and Nanobitechnology*, 1 (1).
  20. Tang, F., Li, L., and Chen, D. (2012) "Mesoporous Silica Nanoparticles: Synthesis, Biocompatibility and Drug Delivery" *Materials Views*, 24, 1504-1534.
  21. Tao, Z., Toms, B., Goodisman, J., and Asefa, T. (2009) "Mesoporosity and Functional Group Dependent Endocytosis and Cytotoxicity of Silica Nanomaterials" *Chem. Res. Toxicol.*, 22,1869–1880.
  22. Vadia, N., and Rajput, S. (2011) "Mesoporous material, MCM-41: A New Drug Carrier" *Asian Journal of Pharmaceutical and Clinical Research*, 4(2), 0974-2441.
  23. Vallet - Regi, M., Balas, F., and Arcos, D. (2007) " Mesoporous Materials for Drug Delivery". *Angew. Chem. Int. Ed.*, 46, 7548 - 7558.
  24. Vallet-Regí, M., Rámila, A., del Real, R., and Pérez-Pariente, J. (2001) "Mesoporous materials for drug delivery" *Chem. Mater.* 13, 308.
  25. Vallet-Regi, M., Doadrio, J. C., Doadrio, A. L., Izquierdo-Barba, I., & Pérez- Pariente, J. (2004). "Hexagonal ordered mesoporous material as a matrix for the controlled release of amoxicillin". *Solid State Ionics*, 72, 435 – 439.
  26. Vallet-Regi, M., Ruiz-Gonzalez, L., Izquierdo-Barba, I., and Gonzalez-Calbet, M. (2006). "Revisiting silica based ordered mesoporous materials: medical applications". *J. Mater. Chem*, 16, 26 - 31.
  27. Wang, S. (2009) "Ordered mesoporous materials for drug delivery." *Microporous Mesoporous Mater*, 117 : 1 - 9.
  28. Zhao, D., Yang, P., Huo, Q., Chmelka, B and Stucky, G. (1998) "Topological Construction of mesoporous materials" *Current Opinion in Solid State and Materials science*; 3, 111-121.
  29. Zhao, H., Yin, L., and Cai, M. (2013) "A Phosphane-Free, Atom-Efficient Cross Coupling Reaction of Triarylbismuths with Acyl Chlorides Catalyzed by MCM-41-Immobilized Palladium Complex" *European Journal of Organic Chemistry*, 2013 (7), 1337–1345.